Deriving connectivity from relatedness: broad-scale isolation-by-distance in the shanny *Lipophrys pholis*

L.-L. Jeannot[1,6,*]**, C. Mouronvalle**[1]**, C. Peyran**[1]**, C. Olabarria**[2]**, M. Beger**[3,4]**,
A. Blanco**[2,3,#]**, S. Planes**[1,5,#]

[1]**PSL Research University, EPHE–UPVD–CNRS, UAR 3278 CRIOBE, 66860 Perpignan, France**
[2]**Centro de Investigación Mariña, Universidade de Vigo, EcoCost, Facultade de Ciencias del Mar,
Edificio CC Experimentais, Campus de Vigo, As Lagoas, Marcosende, 36310 Vigo, Spain**
[3]**School of Biology, Faculty of Biological Sciences, University of Leeds, Leeds LS2 9JT, UK**
[4]**Centre for Biodiversity and Conservation Science, School of Biological Sciences, University of Queensland, Brisbane,
4072 QLD, Australia**
[5]**Laboratoire d'Excellence CORAIL, 66860 Perpignan, France**

[6]*Present address:* **Lancaster Environment Centre, Lancaster University, Lancaster LA1 4YQ, UK**

ABSTRACT: Knowledge about the dispersal patterns of marine organisms is vital for understanding population dynamics and designing appropriately scaled protected areas and fisheries management. Assessing the extent to which populations are connected by larval exchange has been traditionally approached by delineating genetically differentiated populations. Inferring these patterns for species with high gene flow remains a challenge, as they often show panmixia over large spatial scales. In these cases, genetic connectivity may be revealed through the combination of population- and kinship-based approaches. Here, we assess the population structure and relatedness of the shanny *Lipophrys pholis* over 500 km along the Western Iberian Peninsula coastline, using 27 microsatellites developed for this study. As expected, given its long larval duration stage, we found high gene flow throughout the study area. However, a weak pattern of isolation-by-distance was detected by Mantel tests and large-scale relatedness patterns, suggesting decreasing genetic similarity with distance at the scale of the Western Iberian Peninsula. Conversely, we provided evidence of fine-scale connectivity at the smaller scale of the Atlantic Islands of Galicia National Park (Spain). Combining population- and kinship-based approaches may reveal previously undetected genetic differentiation within a well-connected population; however, we stress the importance of careful application and interpretation of relatedness metrics. Our findings may be broadened to other coastal organisms featuring similar life-history traits, including a relatively long larval phase, as well as comparable environmental conditions favoring dispersal by ocean currents, which could be directly applied to the management and conservation of Northeast Atlantic marine species.

KEY WORDS: Gene flow · Relatedness · Isolation by distance · Blenniidae · *Lipophrys pholis*

1. INTRODUCTION

Coastlines are generally composed of a variety of discontinuous habitats which can lead to patchily distributed populations, even in species with highly dispersive life stages (Banks et al. 2007). A large portion of the species inhabiting coastal habitats are either sessile or feature limited movement capabilities as adults; they primarily rely on pelagic dispersal in early life stages for migration between these spa-

tially distant populations, with consequences for critical ecological processes related to population composition and persistence (Cowen et al. 2006, 2007, Cowen & Sponaugle 2009). Understanding how populations are structured and connected is essential to answer key questions underpinning the dynamics of populations (Botsford et al. 2009), to predict how species respond to changing environmental conditions (Hughes et al. 2003, Knutsen et al. 2013), and to design appropriately scaled management units or marine protected areas (MPAs) (Palumbi 2003, Beger et al. 2010, 2015). As one of the main processes shaping population connectivity, larval dispersal has been extensively studied based on pelagic larval duration (PLD) (Shanks 2009), but other biological parameters influence dispersal patterns, including the larval precompetency period (Paris & Cowen 2004), larval behavior (Gerlach et al. 2007, Leis 2007), larval mortality (Cowen et al. 2000), and adult fecundity (Rickman et al. 2000), among others. However, the interaction between these parameters and environmental conditions during dispersal remains poorly understood. In particular, while local connectivity mainly relies on local seascape characteristics and larval biology, the broad-scale exchange of individuals in marine populations is mostly driven by PLD and reproductive output (Bonhomme & Planes 2000, Treml et al. 2012), and can be affected by physical variables such as ocean circulation (Banks et al. 2007, White et al. 2010, Huyghe & Kochzius 2018). Information on the drivers of connectivity between populations and the scale at which they operate is therefore essential to our understanding of population structure and dynamics (Cowen et al. 2006, Dalongeville et al. 2018).

Two approaches are commonly used to assess population structure and are defined as 'population-based' and 'kinship-based' genetic inference methods (Palsbøll et al. 2010). Population-based approaches (such as *F*-statistics [Wright 1949], coalescent methods, and population assignment methods [Pritchard et al. 2000]) are commonly used when allele frequencies are distinct and genetic divergence is large between populations. However, in species with a similar genetic background that either became recently isolated (Landguth et al. 2010, Lloyd et al. 2013) or feature high gene flow (Peery et al. 2008), such methods may not be applicable. When populations have low genetic divergence, kinship-based methods may provide a more suitable alternative, as they compare individual genotypes instead of grouping conspecifics. One widely used kinship-based method is to assign individuals based on the degree of relatedness, which represents genetic similarity as a result of recent shared genealogy or common ancestors (Paetkau et al. 1995, Planes et al. 2009, Saenz-Agudelo et al. 2009, Escoda et al. 2017, Rueger et al. 2020). Kinship-based and population-based methods are complementary, and combining both approaches may improve the ability to identify the contemporary drivers of connectivity, especially in systems with high gene flow (Christie et al. 2010, Iacchei et al. 2013, Schunter et al. 2014, 2019). Kinship-based analyses provide a complementary approach to the analysis of variance in allelic frequencies and potentially useful insights in assessing dispersal within and between MPAs and adjacent areas (Baetscher et al. 2019).

DNA markers such as microsatellites have proven particularly useful in providing relatedness estimates (Blouin et al. 1996). Several estimators have been developed to measure relatedness from molecular marker data when pedigree information is partial or lacking, which is often the case for wild populations. When no prior information can be provided, methods of moments estimators are classically used as opposed to maximum-likelihood methods (Thomas 2005). The moments estimators developed by Queller & Goodnight (1989), Li et al. (1993), Ritland (1996b), Lynch & Ritland (1999), and Wang (2002) are the most common and provide relatedness estimates ranging from −1 to 1, indicating the degree of relatedness between 2 individuals. Estimates can then be used to partition relationships into categories based on expected pedigree relatedness (i.e. 0.5 for parent–offspring, 0.25 for half-siblings, etc.) Here, both relatedness estimates and relationship categories are investigated. Importantly, the estimators' performance varies according to several parameters, including marker set, allele frequency distribution, sampling, and the population being investigated (Van de Casteele et al. 2001, Milligan 2003). The importance of good-quality markers has been stressed, specifically in the context of populations presenting weak structure, which have been suggested to necessitate highly polymorphic markers (Ritland 1996a). Marker quality is essential to reduce rates of false-positive or false-negative assignments (i.e. 2 unrelated individuals identified as full-siblings, half-siblings, or parent–offspring and inversely) (Wilson & Ferguson 2002, Jones et al. 2010). However, minimizing false-positive rates (FPR) usually comes at the cost of reducing the number of assignments and is a notorious challenge in parentage analysis (Jones et al. 2010, Harrison et al. 2013a,b). The accuracy of assignments may also depend on the relationship category, with half-

siblings often being less reliable than full-siblings or parent–offspring relationships (Melero et al. 2017), which may lead to underpowered studies (Baetscher et al. 2018). Conversely, half-sibling relationships are commonly found in parentage analysis for wild populations of polygamous species (Nance et al. 2011) and are particularly interesting as a complement to full-siblings in the context of large effective population sizes and group reproductive behavior, for which full-siblings occur at smaller frequencies (Wang 2009).

The shanny *Lipophrys pholis* (Linnaeus, 1758) is a small, abundant fish commonly found in intertidal rockpools throughout the Northeast Atlantic (Gibson 1982). Its distribution extends from Scotland to Morocco, and from the Azores and Madeira to the western Mediterranean Sea (Zander 1986). Once settled, juveniles migrate among pools relative to their size within the same area as they grow (Faria & Almada 2001, Monteiro et al. 2005). Adults are characterized by high site fidelity, which they recognize through navigational cues (Jorge et al. 2012, Martins et al. 2017). In the study area, spawning starts from early autumn to late spring (Almada et al. 1990, Faria et al. 1996), after which demersal eggs hatch and larvae disperse along the coast for a long PLD of 57–73 d (Carvalho et al. 2017a). As larval dispersal is the only life stage connecting geographically distant populations, this species is a good model with which to analyse dispersal patterns. Limited population structure along *L. pholis*' range has already been described using both mitochondrial (control region, D-Loop, 12S, and 16S) and nuclear (S7) genetic markers, with one population spanning the European coast from the UK to Morocco, and another one in the Azores (Francisco et al. 2006, 2011, Stefanni et al. 2006). However, *L. pholis* otoliths' geochemical tracers revealed low dispersal at the scale of Portugal but overlapping isotopic signatures between geographically close sampling sites, suggesting genetic homogeneity due to significant movement of juveniles and/or larval retention at a finer scale (Carvalho et al. 2017b). This increase in difference with geographic scale suggests a possible pattern of isolation-by-distance (IBD) (Slatkin 1987, 1993). However, so far, genetic variability in this region could only be detected among sampling years, indicating some level of temporal genetic heterogeneity in the shanny shaped by interannual oceanographic fluctuations (Francisco & Robalo 2015, 2020); no evidence of spatial genetic heterogeneity at the scale of the Portuguese coast exists as of yet.

Genetic approaches more suited to the study system can provide additional knowledge about the population structure of *L. pholis* in the sampled area and complement previously used methods. Here, we aimed to characterize population structure and connectivity at both large (>500 km) and fine (50 km) scales in an *a priori* well-connected population of the shanny *L. pholis*, using both population-based approaches and kinship-based relatedness estimates inferred from microsatellite genotypes. Specifically, we evaluated the role of geographic distance in shaping population structure. We highlight that combining population-based and kinship-based analyses can shed some light on connectivity patterns, and we stress that high gene-flow species require careful application and interpretation of genetic approaches to better understand population connectivity.

2. MATERIALS AND METHODS

2.1. Study system and sampling

A total of 519 *Lipophrys pholis* were collected from June 2019 to October 2020, using hand nets in rock pools along the Spanish and Portuguese coast at 16 sampling sites separated by 5–522 km. The fish were taken to the laboratory for morphological identification (Almeida 1985). Given the 6–10 yr lifespan of *L. pholis* (Dunne 1977, Carvalho et al. 2017c), individuals were considered as belonging to the same cohort and were pooled together for further analysis (Fig. S1 in the Supplement at www.int-res.com/articles/suppl/m731p009_supp.pdf). Fin clip samples were preserved in 70% ethanol until DNA extraction (see Table 1 for additional collection information). Two spatial scales were studied: first, we investigated a large geographic scale corresponding to the entire study area, extending from Galicia (42° 34' 33.0" N, 9° 5' 28.8" W) to the northern coast of the Alentejo region (37° 52' 21.1" N, 8° 47' 45.2" W) in southern Portugal, covering over 500 km of coastline. The Western Iberian Peninsula features deep indentations in the Galician coastline, followed by a generally rectilinear coastline oriented in the NNW–SSE direction, and is dominated by a succession of rocky shores and sandy beaches. We drew specific focus to the stretch of coastline spread over 50 km situated in Galicia, Spain, which encompasses the MPA Atlantic Islands of Galicia National Park, allowing us to investigate connectivity between 4 islands of the MPA (from north to south: Sálvora, Ons, Cies Island North, and Cies Island South) and their neighbouring areas (Fig. 1).

All sampling procedures were in accordance with Spanish (Royal Executive Order, 53/2013) and Euro-

Table 1. Collection information for the 16 sampling sites ordered from north to south. N corresponds to the number of sampled *Lipophrys pholis*. Shaded rows indicate that the sampling site is located within one of the MPAs of the Atlantic Islands of Galicia National Park

| Site	Location	Country	N	Latitude	Longitude
Cor	Corrubedo	Spain	38	42° 34′ 33.0″ N	9° 05′ 28.8″ W
Salv	Sálvora	Spain	32	42° 28′ 45.8″ N	9° 01′ 06.8″ W
Grove	O Grove	Spain	38	42° 27′ 48.8″ N	8° 56′ 34.8″ W
Ons	Ons Island	Spain	42	42° 23′ 28.4″ N	8° 55′ 24.0″ W
Cous	Couso Cape	Spain	39	42° 18′ 31.6″ N	8° 51′ 26.1″ W
CiesN	Cies Island North	Spain	35	42° 14′ 16.3″ N	8° 54′ 04.0″ W
CiesS	Cies Island South	Spain	30	42° 11′ 35.6″ N	8° 53′ 46.5″ W
Sil	Silleiro Cape	Spain	28	42° 06′ 40.7″ N	8° 54′ 00.7″ W
Via	Viana Castelo	Portugal	25	41° 41′ 52.6″ N	8° 51′ 11.3″ W
Espo	Esposende	Portugal	38	41° 34′ 26.6″ N	8° 47′ 57.8″ W
Fig	Figueira de Foz	Portugal	30	40° 10′ 38.5″ N	8° 54′ 08.3″ W
Ber	Berlengas Islands	Portugal	23	39° 24′ 37.8″ N	9° 30′ 49.6″ W
Eri	Ericeira	Portugal	37	38° 59′ 24.9″ N	9° 25′ 20.2″ W
Ave	Avencas	Portugal	37	38° 41′ 10.7″ N	9° 21′ 26.4″ W
Ses	Sesimbra-Arrábida	Portugal	30	38° 26′ 19.8″ N	9° 05′ 14.6″ W
Sin	Sines	Portugal	17	37° 52′ 34.9″ N	8° 47′ 43.7″ W
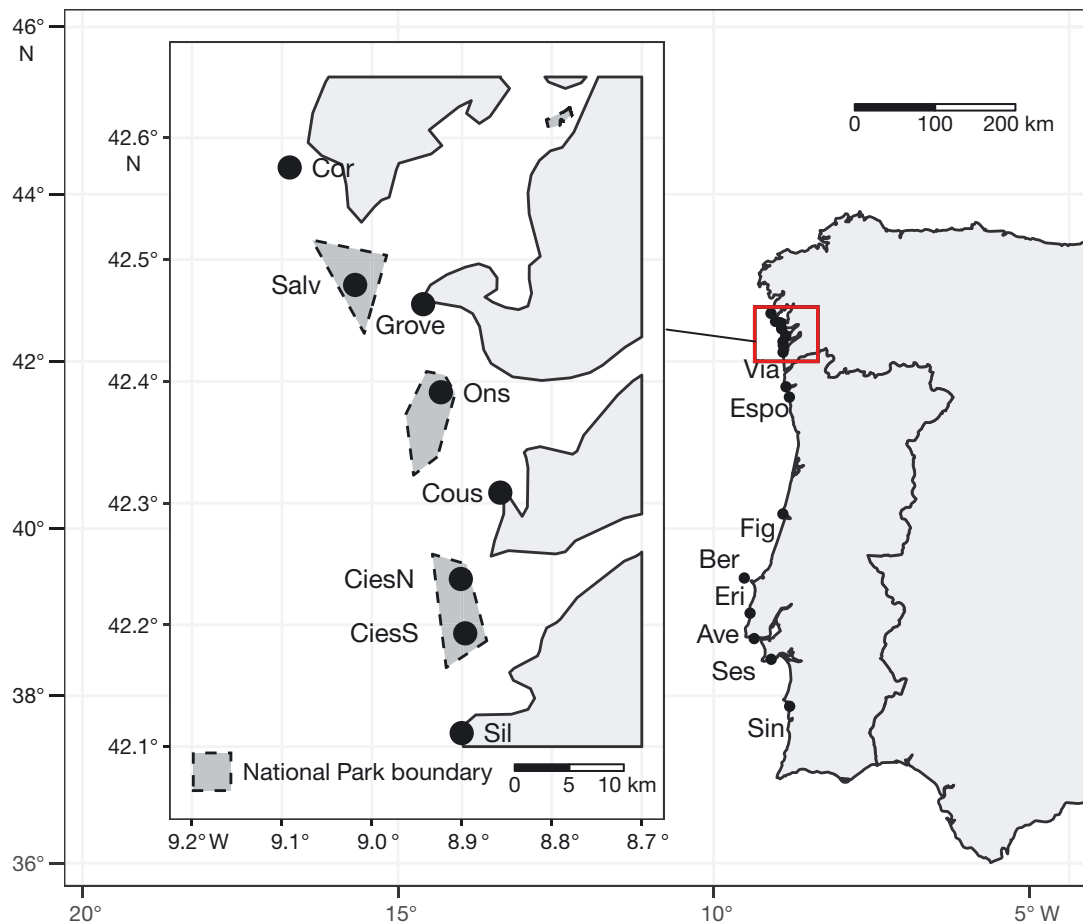
Fig. 1. Sampling sites in Spain (Cor, Salv, Grove, Ons, Cous, CiesN, CiesS, Sil) and Portugal (Via, Espo, Fig, Ber, Eri, Ave, Ses, Sin). The rectangle indicates sites chosen for small-scale analysis. Sites correspond to the following locations: Corrubedo, Sálvora, O Grove, Ons Island, Couso Cape, Cies Island North, Cies Island South, Silleiro Cape, Viana Castelo, Esposende, Figueira de Foz, Berlengas Islands, Ericeira, Avencas, Sesimbra-Arrábida, and Sines

pean (European Union Directive 2010/63/UE, Article 9) Laws for animal experimentation, and were explicitly authorized by local authorities from both countries, under permit number RX95169 for sampling sites located in Spain and permit number 29386/2020/DR-LVT/DCNB/DPL for those located in Portugal.

2.2. Molecular analyses

Genomic DNA was extracted using the QIAamp® 96 DNA QIAcube® HT robot workstation (Qiagen). DNA templates were then diluted at 50 ng μl^{-1} and stored at −24°C. Genotyping was performed on all 519 samples, using a set of 27 microsatellite markers developed for *L. pholis* (Jeannot et al. 2022), with identical PCR conditions.

2.3. Genetic diversity

The presence of null alleles, large allele dropout, and scoring errors were tested in the newly developed set of markers using MICRO-CHECKER (van Oosterhout et al. 2004). Using GENALEX v.6.503 (Peakall & Smouse 2006, 2012), we explored genetic diversity for each sampling site by computing the allelic richness (N_a), the number of private alleles (N_p), and expected and observed heterozygosities (H_e and H_o, respectively). Since sample sizes ranged from 17 to 42, the program ADZE was used to calculate standardized allelic richness (A_r) and standardized private allelic richness (A_{pr}) based on the smaller sample size (Szpiech et al. 2008). The inbreeding coefficient F_{IS} was computed for all loci and sampling sites using the Weir and Cockerham method (Weir & Cockerham 1984) implemented in the GENETIX software (Belkhir et al. 1996), and the significance of values was assessed by permutations (1000 permutations per population).

2.4. Genetic structure

2.4.1. Population-based approach

Genetic structure was investigated through a Bayesian model-based clustering method implemented in STRUCTURE v.2.3.4 (Pritchard et al. 2000). The model was run with no prior information about sampling location and with a burn-in period of 50 000 iterations, followed by 100 000 Monte Carlo Markov chain

replicates for 1–16 clusters and with 10 iterations for each number of cluster (Evanno et al. 2005). STRUCTURE HARVESTER online (Earl & vonHoldt 2012) was used to compute an ad hoc statistic (ΔK) to choose the optimal cluster number. Further exploration of genetic structure was done using a principal coordinates analysis (PCoA) computed on GENALEX to detect possible partitioning among sampling sites.

To explore IBD while accounting for spurious correlations associated with traditional Mantel tests (Guillot & Rousset 2013, Legendre et al. 2015), a Moran spectral randomization (MSR) procedure was implemented as described in Crabot et al. (2019). This spatially constrained permutation method generates randomized replicates while preserving the spatial structure of samples, thus correcting for spatial autocorrelation while maintaining the ability to detect true correlations between genetic and geographic distance. As IBD results may be sensitive to the choice of genetic distance measure (Séré et al. 2017), we tested the effect of 2 common measures: linearized fixation index, F_{ST} ($F_{ST}^* = 1 / [1 - F_{ST}]$) and Nei's genetic distances (Nei 1972, Rousset 1997). While F_{ST} is not a genetic distance stricto sensu but a measure of relative genetic variance of subsamples as compared to the total sample, it remains one of the most fundamental metrics of population structure and can be particularly useful in case of high gene flow (Balloux & Goudet 2002). The MSR–Mantel procedure was implemented using the 'msr' function from the R package 'adespatial' on Mantel test outputs with 999 random replicates (Dray et al. 2022). Standardized effect sizes (SES) were computed by dividing the corrected Mantel statistic by the standard deviation of MSR replicates (Gotelli & McCabe 2002, Crabot et al. 2019). F_{ST} was calculated between sites using the Robertson and Hill estimator implemented in GENETIX with the Raufaste and Bonhomme correction, which is more appropriate for low F_{ST} values (<0.05) (Robertson & Hill 1984, Raufaste & Bonhomme 2000). The p-values were then corrected using the Holm-Bonferroni sequential correction. Matrices of Nei's genetic distance between sites were calculated using GENALEX. Geographic distance between sampling sites was defined using 2 methods: straight-line distances and least-cost path distances, which correspond to the shortest path to reach one site from another while avoiding land. Straight-line distances were computed using the R package 'geosphere' based on the haversine method (Sinnott 1984, Hijmans 2021a). Least-cost path distances were obtained using land maps from Spain and Portugal, which were rasterized (resolution: 0.1 degrees) with the

'rasterize' function of the 'raster' package implemented in R (Hijmans 2021b). The 'costDistance' function from the 'gdistance' package was used to compute the least-cost path between each pair of sites (van Etten 2017), following the methodology presented in Van Wynsberge et al. (2017).

2.4.2. Kinship-based approach

Given that relatedness estimators' performance varies according to marker set and sample population, we used the R package 'related' to select the best-suited relatedness estimator for our case study (Csilléry et al. 2006, Pew et al. 2015). We conducted a first set of simulations of known relatedness (1000 dyads each of parent–offspring, full-siblings, half-siblings, and unrelated individuals) assuming an error rate of 0.002 for all loci and allowing for inbreeding, with an error rate based on repeat genotyping of ~10% of the data (50 randomly selected individuals) based on the set of 27 microsatellites developed by Jeannot et al. (2022). Expected relatedness values were generated based on allele frequencies within our sample. Expected relatedness was then compared to estimated relatedness using Pearson's correlation coefficient to test the performance of 4 commonly used estimators: *Lynch-Li* (Li et al. 1993), Lynch-Ritland (Lynch & Ritland 1999), Queller-Goodnight (Queller & Goodnight 1989), and *Wang* (Wang 2002, 2007). Three out of the 4 estimators performed equally well, with similar correlation coefficients of >0.95 (*Lynch-Li*: 0.953; Queller-Goodnight: 0.950; *Wang*: 0.954); the Lynch-Ritland estimator appeared slightly less adapted (0.88) (Fig. S2 in the Supplement). All 4 markers were used to compare relatedness estimates, and the Lynch-Li estimator *Lynch-Li*, the Lynch-Ritland estimator l_{xy}, the Queller-Goodnight estimator r_{xy}, and the Wang estimator *Wang* were computed for all pairs among the 519 individuals using the R package 'Demerelate' (Kraemer & Gerlach 2017).

For assignment into relationship categories, we chose to rely on the Queller-Goodnight estimator, given its widespread use in numerous other fish species (Buston et al. 2007, 2009, Schunter et al. 2011, 2019, D'Aloia et al. 2018, Rueger et al. 2020, 2021). Individuals with a coefficient $r_{xy} > 0.25$ were assumed to have at least one parent in common (i.e. half-siblings), while a coefficient $r_{xy} > 0.5$ typically corresponds to 2 common parents (full-siblings) (Oliehoek et al. 2006). Lower r_{xy} thresholds may correspond to more distantly related or unrelated individuals; how-

ever, overlapping expected r_{xy} distributions of different relationship categories (i.e. unrelated, half-siblings, full-siblings, and parent–offspring) may make classification of pairs into these categories difficult (Csilléry et al. 2006, Taylor 2015). As such, a second set of simulations was conducted to determine confidence in assignments. We used the package 'CKMR-sim' (Anderson 2023), which uses Monte Carlo simulations of individuals of known relatedness (parent–offspring, full-siblings, half-siblings, and unrelated individuals) to generate expected log-likelihood ratio distributions for each relationship category along with FPRs and false-negative rates (FNRs) associated with each previously identified relationship. We used our sample's allele frequencies and an identical genotyping error rate of 0.002 as for the previous set of simulations, and 10 000 dyads each of parent–offspring, full-siblings, half-siblings, and unrelated individuals were simulated. As no value was found with a coefficient $r_{xy} > 0.5$, we focused on half-sibling relationships and visualized the expected overlap in relatedness distributions between half-siblings and unrelated individuals (Fig. S3 in the Supplement). We selected a log-likelihood ratio threshold of 1, corresponding to an FPR of 0.76×10^{-2} and an FNR of 3.12×10^{-2}, below which relationships were excluded from further analysis. Although higher log-likelihood ratio cut-off values have been proposed for increased accuracy (Baetscher et al. 2018, Anderson 2023), this threshold was chosen to balance the number of relationships used for analysis with correct assignment rate, a trade-off that is typical in parentage analyses (Harrison et al. 2013a). To observe the effect of raising the log-likelihood ratio thresholds and thereby applying more stringent FPRs, a sensitivity analysis was conducted. Higher log-likelihoods values ranging from 2 to 6 (for which only 2 relationships remained for broad-scale analysis and 1 for small-scale analysis) were used to assign relationships to either unrelated or half-sibling categories. Details of the sensitivity analysis, including the corresponding number of relationships identified as half-siblings, FPRs, and FNRs are presented in Table S1 in the Supplement.

To identify large-scale relatedness patterns, relatedness estimates were averaged and relationships were counted for all combinations of the 16 sampling sites spanning over 500 km of coastline, amounting to 136 combinations. To investigate relatedness patterns at the scale of a network of MPAs and their neighboring areas, 8 sampling sites, each separated by less than 50 km in Galicia, were considered for small-scale analysis, totaling 36 combinations. In both cases, for each of the 4 estimators, normality

was tested using a Shapiro-Wilk test. Average relatedness was compared between small-scale and broad-scale sites using t-tests when relatedness values distribution was normal (r_{xy}, *Wang*, *Lynch-Li*) and using a Wilcoxon test otherwise (l_{xy}). The MSR–Mantel procedure was applied to relatedness estimates, but not to the number of half-siblings, as the MSR–Mantel procedure is not applicable to count data. In the latter case, to explore the relationship with distance, we used a generalized linear model regression with geographic distance as an explanatory variable of the number of half-siblings, using the R package 'glmmTMB' (Brooks et al. 2017). In line with MSR–Mantel analyses, we also tested 2 different distance variables as predictors (straight-line distances and least-cost path distances) and explored large-scale and small-scale relatedness patterns. Negative binomial models with quadratic parametrization were used to account for overdispersion. The 4 resulting models were compared to their corresponding null models (no relationship between number of related individuals and geographic distance), and a best-fit model was chosen using the lowest Akaike's information criterion (AIC) value (Sakamoto et al. 1986). R^2 was computed based on the likelihood-ratio test implemented in the 'MuMIn' package (Barton 2020), and statistical significance was evaluated at the $\alpha = 0.05$ threshold to determine whether a more stringent value could influence the relationship with distance. For each cut-off value, the same modelling procedure was applied, with the exception of relationships with a log-likelihood of 6 and above, for which a Poisson model was fitted, as the negative binomial did not converge. All R analyses were done using R v.4.2.1 and RStudio v.4.0.3 (R Core Team 2020).

3. RESULTS

3.1. Marker set and genetic diversity

Of the 27 markers that were investigated, MICRO-CHECKER did not detect evidence of null alleles, scoring errors, or large allele dropout. Markers presented varying levels of polymorphism, ranging from an average of 7.4 alleles per locus to 30.8, with an overall average ($\pm$SD) of 18 ± 6.3 alleles. H_o

ranged from 0.640 to 0.963, with an average of 0.866 $\pm$ 0.082, and H_e varied in the same range as H_o, from 0.635 to 0.951, with an average of 0.870 $\pm$ 0.078 (Table S2 in the Supplement). Overall, 11 out of 27 markers presented a low but significant F_{IS} in 1–6 sampling sites out of 16 sampling sites (Table S3 in the Supplement), demonstrating limited heterozygote deficiency and deviation from the Hardy-Weinberg equilibrium.

Genetic analyses revealed a high level of polymorphism in each sampled site, with high mean N_a per sampling site, ranging from 14.29 to 20.07 with an average of 17.97 (Table 2). N_p ranged from 2 to 15. A_r ranged from 8.83 to 10.09, and A_{pr} ranged from 0.31 to 0.44. H_o ranged from 0.843 to 0.893, with an average of 0.866 $\pm$ 0.015, while H_e ranged from 0.876 to 0.898, with a slightly higher average of 0.884 $\pm$ 0.006. Nine out of 16 sampling sites exhibited a weak but significant F_{IS} for 1–6 out of 27 markers (Table S3).

When focusing on the 8 sampling sites used to investigate patterns at the smaller scale of an MPA network, genetic diversity indices did not differ significantly between sites within the Atlantic Islands of Galicia National Park (average $H_e = 0.88 \pm 0.003$; average $H_o = 0.862 \pm 0.009$) and sites located outside of the MPA (average $H_e = 0.885 \pm 0.002$; average $H_o = 0.857 \pm 0.016$).

Table 2. Summary statistics of genetic diversity index for each sampling site. H_e: expected heterozygosity; H_o: observed heterozygosity; N_a: allelic richness; N_p: number of private alleles; A_r: standardized allelic richness; A_{pr}: standardized private allelic richness; F_{IS}: fixation index. Sites are ordered from north to south corresponding to the following locations: Corrubedo, Sálvora, O Grove, Ons Island, Couso Cape, Cies Island North, Cies Island South, Silleiro Cape, Viana Castelo, Esposende, Figueira de Foz, Berlengas Islands, Ericeira, Avencas, Sesimbra-Arrábida, and Sines

	H_e	H_o	N_a	N_p	A_r	A_{pr}	F_{IS}
Cor	0.885	0.88	19.3	11	9.68	0.4	0.006
Salv	0.876	0.861	18.3	5	9.66	0.35	0.018
Grove	0.886	0.843	19.3	9	9.79	0.39	0.049
Ons	0.883	0.875	20.1	10	9.78	0.42	0.009
Cous	0.887	0.858	19.9	9	9.8	0.41	0.033
CiesN	0.882	0.856	17.9	8	9.65	0.36	0.03
CiesS	0.88	0.856	17.1	9	9.46	0.31	0.028
Sil	0.882	0.848	16.8	10	9.65	0.37	0.039
Via	0.885	0.866	16.4	4	9.79	0.37	0.021
Espo	0.881	0.869	18.9	7	9.63	0.32	0.014
Fig	0.884	0.892	17.8	8	9.79	0.36	−0.009
Ber	0.898	0.868	17	10	10.09	0.39	0.035
Eri	0.89	0.894	18.6	12	9.83	0.39	−0.004
Ave	0.884	0.857	18.4	6	8.83	0.35	0.031
Ses	0.882	0.875	17.5	15	9.64	0.44	0.009
Sin	0.885	0.855	14.3	2	9.8	0.34	0.035
Average	0.884	0.866	18	8	9.68	0.37	0.021

3.2. Large-scale population structure and genetic differentiation

All pairwise F_{ST} values were low (ranging from 0.0026 to 0.02063) and non-significant after the Holm-Bonferroni correction (Table S4 in the Supplement). No partitioning between sites was detected through the PCoA based on Nei's genetic distance (Fig. 2). The Bayesian model-based clustering analysis identified 2 clusters based on Evanno's method, which is the lowest number of possible clusters (Fig. S4 in the Supplement). However, individuals were not assigned to a distinct cluster and there was a high level of admixture, and overall no relationship between clusters and spatial distribution could be evidenced (Fig. S5 in the Supplement). Genetic distances appeared correlated to distances between sites, with linear regression evidencing a significant effect of geographic distance both for $F_{ST}*$ and Nei's genetic distances (Fig. 3). In line with this observation, the MSR–Mantel test performed on the entire data set revealed weak but significant structuring of $F_{ST}*$ genetic distances by geographic distances, both when distances were computed using straight lines ($r_{MSR} = 0.047$, SES = 2.28, p = 0.027) or least-cost path ($r_{MSR} = 0.059$, SES = 2.04, p = 0.015). Interestingly, the MSR–Mantel procedure showed a correlation between Nei's genetic distances and geographic distances when using straight-line distances ($r_{MSR} = 0.049$, SES = 2.09, p = 0.018) but not with least-cost path distances ($r_{MSR} = 0.062$, SES = 1.69, p = 0.053) (Table 3).

Average relatedness was low regardless of the choice of estimator and was between $-2.74 \times 10^{-3} \pm 0.06$ (*Wang*) and $-1.56 \times 10^{-3} \pm 0.07$ (*Lynch-Li*). Regression showed a significant negative effect of distance on average relatedness when using the Lynch-Ritland estimator l_{xy} but, while slopes were negative for all other estimators, the effect of distance was not found to be significant (Figs. 3 & S6 in the Supplement). Furthermore, no significant relationship with distance was found when applying the MSR correction to Mantel tests (Table 3). Of the 134 421 relationships evaluated, 33 had $r_{xy} > 0.25$ (0.025 %), with the highest r_{xy} value equaling 0.31. Log-likelihood for all samples ranged from −18.4 to 9.2, with an average of −7.8, further suggesting overall low relatedness among sampled individuals. Among relationships with $r_{xy} > 0.25$, log-likelihood ratios ranged from −0.4 to 7.3. After correcting for FPRs by selecting relationships with a log-likelihood of >1, 25 relationships remained (0.019 %). The number of relationships between sampling sites varied between 0 and 2, with an average of 0.2 relationships. Overall, the models
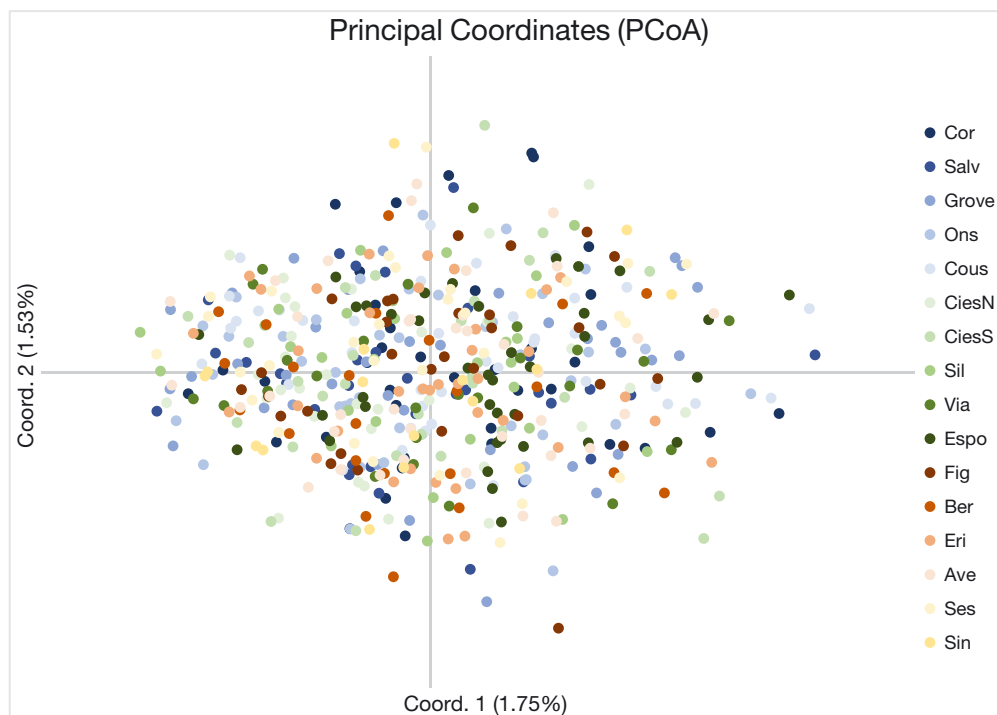

Fig. 2. Principal coordinates analysis (PCoA) generated in GenAlEx using Nei's genetic distance matrix. Coordinate axis 1 explains 1.75 % of total variation, and coordinate axis 2 explains 1.53 % of total variation. Sites are ordered from north to south
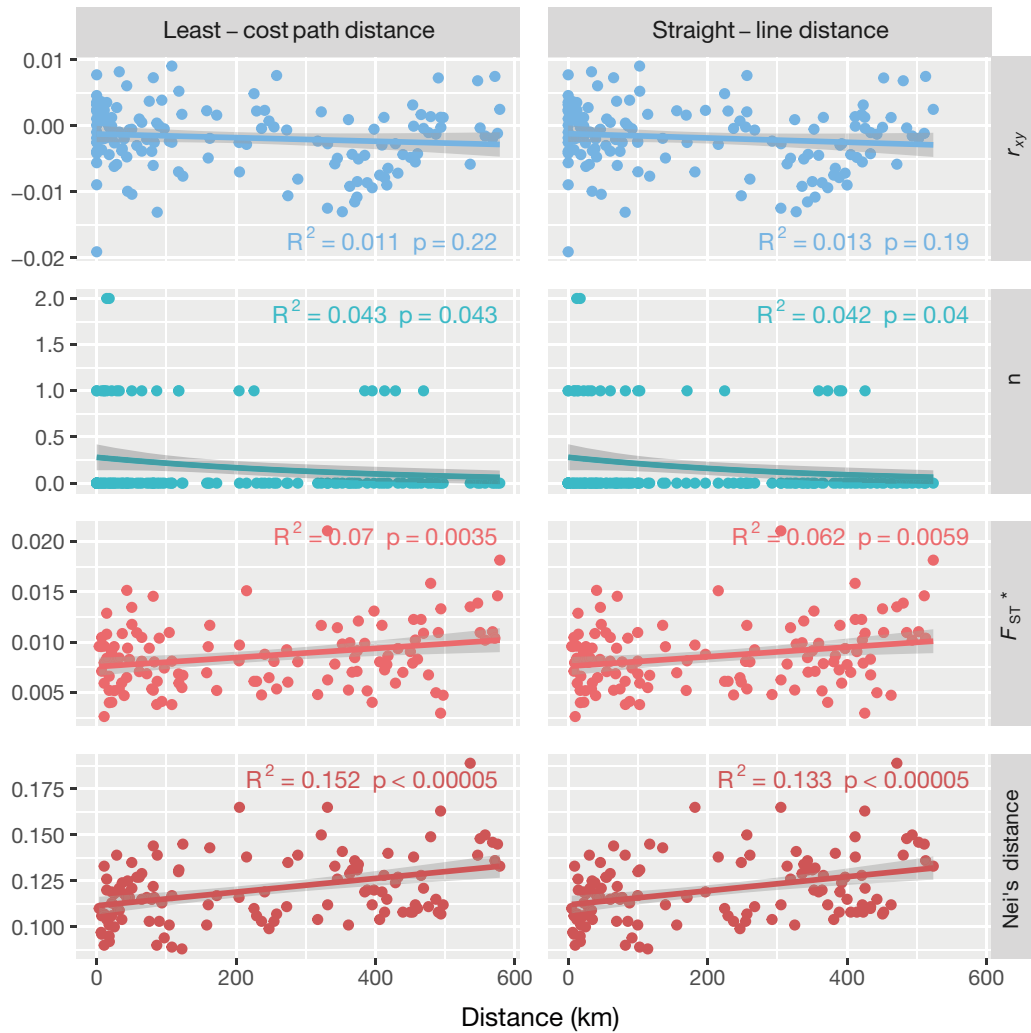
Fig. 3. Relatedness estimates (relative relatedness: r_{xy}, Queller & Goodnight 1989; number of half-sibling relationships, n, based on log-likelihood >1) and population-based estimates (F_{ST}^*; Nei's genetic distance, Nei 1972, Rousset 1997) according to geographic distance. R^2 and p-values for r_{xy}, F_{ST}^*, and Nei's genetic distance are computed based on linear regressions. R^2 and p-value for n are based on a negative-binomial model for which results are detailed in Tables 4 & S4. Shaded bands: 95% CI

featuring distance as an explanatory variable performed better than null models, and models with least-cost path distances did not present a better fit than models using straight-line distances. The results for the 2 distance models are presented in Table 4 and plotted in Fig. 3 (see detail in Table S5 in the Supplement). Overall, the regression indicates a small but significant contribution of geographic distances in explaining the number of relationships, both for least-cost path distances (R^2 = 4.26%, p = 0.043) and for straight-line distances (R^2 = 4.18%, p = 0.040).

Similar results were obtained when raising the log-likelihood threshold to 3, thereby decreasing the FPR to 1.67×10^{-4} and reducing the number of half-sibling relationships to 12. However, for all thresh-

olds above 4, the relationship between the number of relationships with distance was no longer significant. Compared to the null model, the model including either least-cost path or straight-line distances performed better in almost all cases, up until the model with a log-likelihood of >6 with only 2 half-sibling relationships, which featured comparable AIC for the geographic distance and null models (Tables 4 & S5). Interestingly, out of the 25 relationships identified with a log-likelihood of >1, the closest relationships displayed higher log-likelihoods than distant ones (Fig. 4), suggesting that the half-sibling relationships identified with the highest level of confidence were the closest ones. Full sensitivity analysis details are presented in Table S5.

Table 3. MSR–Mantel (r_{MSR}) test results. LC-distance: least-cost path; SL-distance: straight-line distance. SES: standardized effect size; $F_{ST}^\star$: linearized F_{ST}; r_{xy}: Queller-Goodnight estimator; l_{xy}: Lynch-Ritland estimator. *p < 0.05

Scale	Matrix 1	Matrix 2	SES	p	r_{MSR}
Large	Nei	LC-distance	1.69	0.053	0.062
		SL-distance	2.09	0.018*	0.049
	$F_{ST}^\star$	LC-distance	2.04	0.015*	0.059
		SL-distance	2.28	0.027*	0.047
	r_{xy}	LC-distance	−1.06	0.868	−0.041
		SL-distance	−0.94	0.819	−0.032
	Wang	LC-distance	0.8	0.192	0.02
		SL-distance	0.97	0.155	0.024
	Lynch-Li	LC-distance	−0.75	0.766	−0.022
		SL-distance	−0.54	0.673	−0.015
	l_{xy}	LC-distance	−1.17	0.877	−0.07
		SL-distance	−1.1	0.831	−0.067
Small	Nei	LC-distance	0.76	0.21	0.063
		SL-distance	0.93	0.153	0.077
	$F_{ST}^\star$	LC-distance	0.86	0.184	0.063
		SL-distance	0.76	0.195	0.055
	r_{xy}	LC-distance	0.69	0.218	0.05
		SL-distance	0.97	0.169	0.062
	Wang	LC-distance	−0.15	0.505	−0.011
		SL-distance	0.14	0.387	0.009
	Lynch-Li	LC-distance	−0.65	0.736	−0.033
		SL-distance	−0.13	0.5	−0.006
	l_{xy}	LC-distance	−0.27	0.581	−0.018
		SL-distance	−0.07	0.487	−0.005

3.3. Fine-scale population structure and genetic differentiation

When considering the 8 sampling sites from the Atlantic Islands of Galicia National Park and its surroundings, no patterns of relationship between geographic and genetic distances were evidenced with the MSR–Mantel test. Nei's genetic distances were independent of both straight-line distances (r_{MSR} = 0.077, SES = 0.93, p = 0.153) and least-cost path distances (r_{MSR} = 0.063, SES = 0.76, p = 0.21). When using $F_{ST}^\star$ as a measure of genetic distance, no correlation was found with either straight-line distances (r_{MSR} = 0.055, SES = 0.76, p = 0.195) or least-cost path distances (r_{MSR} = 0.063, SES = 0.86, p = 0.184). MSR–Mantel tests performed on relatedness values equally showed a lack of correlation between average relatedness values and geographic distance (Table 3). Average relatedness of all sites included in the fine-scale analysis was low, although slightly higher than when including all sites, and ranged between $−4.51 \times 10^{-4} \pm 0.07$ (Lynch-Li) and $−27.19 \times 10^{-4} \pm 0.06$ (Wang). The difference in relatedness between fine-scale and broad-scale sites was consistent among all estimators, suggesting that individu-

als from the sites situated within the MPA and separated by a maximum of ~50 km were more related than individuals from distant sites (Fig. 5). However, a significant difference was revealed only when using the Queller-Goodnight r_{xy} estimator (t = −2.36, p = 0.011). Concerning related relationships, out of 39 621 combinations, 10 relationships with $r_{xy} > 0.25$ and log-likelihood > 1 were found for small-scale analysis (0.025 %). The number of relationships with $r_{xy} > 0.25$ between sampling sites in Galicia varied between 0 and 1, with an average of 0.28 relationships. The models using either type of distance as an explanatory variable did not perform better than the null model, regardless of log-likelihood cutoff value (Table 4).

4. DISCUSSION

Accurately detecting spatially driven population structuring is key to better understand processes driving species' ecology and evolution, but also to implement ecologically driven conservation strategies. Here, we showed that combining several methods across multiple spatial scales to infer population structure and connectivity can reveal underlying patterns of genetic differentiation even in species with potentially high gene flow, where signals of differentiation are weaker. In particular, we showcased that kinship analysis through relatedness estimates can be useful to assess realized dispersal events between sites, and provides fine-scale information on connectivity and structure which can complement other approaches (i.e. population-based approaches), even in the case of samples with few related individuals. However, the weakness of these patterns illustrates the challenges associated with kinship analysis and the difficulty of identifying differentiation in high gene-flow species. As such, we draw particular attention to methodological caveats associated with accurately assessing patterns of genetic differentiation in such cases.

In this paper, we found limited but significant genetic structuring according to geographic distance throughout the Western Iberian Peninsula coastline. This pattern appears detectable at a large scale only, as no such differentiation was found when considering the smaller scale of the Atlantic Islands National Park. In line with previous genetic analyses investigating the population structure of *Lipophrys pholis* (Francisco et al. 2006, 2011, Stefanni et al. 2006), we found high and homogeneous genetic diversity, and no clear genetic partitioning was observed. Several loci (11 out of

Table 4. Distance generalized linear model results and fit comparison. LC-distance: least-cost path; SL-distance: straight-line distances. An explanatory value of 1 corresponds to the null model. p-values correspond to the significance of the effect of the distance variable; *p < 0.05. AIC: Akaike's information criterion. Full model results are presented in Supplementary Table S5

Log-likelihood cutoff	Scale	Explanatory variable	p	AIC	Dispersion	R^2 (%)
1	Large	LC-distance	0.043*	138.66	0.937	4.26
		SL-distance	0.04*	138.7	0.94	4.18
		1	–	140.87	0.991	0
	Small	1	–	52.09	1.019	0
		SL-distance	0.889	54.07	1.015	0.06
		LC-distance	0.913	54.08	1.017	3.91×10^{-2}
2	Large	SL-distance	0.015*	104.61	1.003	9.22
		LC-distance	0.015*	104.66	0.995	9.29
		1	–	110.74	0.997	0
	Small	1	–	49.03	0.993	0
		LC-distance	0.968	51.03	0.994	0.55×10^{-2}
		SL-distance	0.97	51.03	0.991	0.47×10^{-2}
3	Large	SL-distance	0.034*	82.59	0.949	8.15
		LC-distance	0.034*	82.64	0.933	8.22
		1	–	87.29	1.006	0
	Small	1	–	38.44	1.018	0
		SL-distance	0.844	40.4	1.005	0.13
		LC-distance	0.905	40.42	1.013	4.92
4	Large	SL-distance	0.059	64.08	0.585	18.5
		LC-distance	0.059	64.23	0.596	18.26
		1	–	71.17	0.992	0
	Small	1	–	34.19	0.987	0
		SL-distance	0.742	36.07	0.958	0.42
		LC-distance	0.825	36.14	0.974	0.19
5	Large	SL-distance	0.106	50.02	0.634	9.07
		LC-distance	0.107	50.15	0.643	8.87
		1	–	53.45	0.97	0
	Small	1	–	34.19	0.971	0
		SL-distance	0.533	36.07	0.902	1.46
		LC-distance	0.582	36.14	0.919	1.13
6	Large	SL-distance	0.356	22.77	0.599	4.51
		LC-distance	0.356	22.77	0.599	4.64
		1	–	22.88	1	0
	Small	1	–	11.17	1.029	0
		SL-distance		13.16	1.028	0.94×10^{-2}
		LC-distance	0.989	13.17	1.029	6.93×10^{-6}

27) showed evidence of heterozygote deficiency for a few sampling sites, which can be related to the presence of null alleles in low frequency, inbreeding, selection, or a Wahlund effect (see Jeannot et al. 2022 for further discussion). However, both inbreeding and a Wahlund effect would be observed at all loci, and no markers with signs of null alleles were detected. In addition, no locus presented consistent patterns of significant F_{IS} at all for most sampling sites, suggesting that this set of markers was appropriate for further analysis. As such, all 27 loci were retained for the analyses presented here.

4.1. High gene flow

Understanding the drivers of population connectivity and the scale at which they operate is key for the effective conservation and management of wild populations. Here, we documented patterns of small- and large-scale gene exchange throughout the Western Iberian Peninsula in the shanny *L. pholis* based on the combined use of population-based and kinship-based approaches. Similar to previous genetic analyses (Francisco et al. 2006, 2011, Stefanni et al. 2006), population-based approaches support the
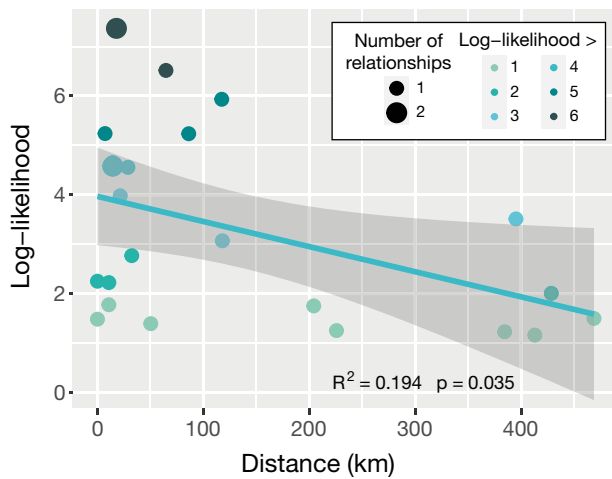
Fig. 4. Log-likelihoods of half-sibling relationships identified with $r_{xy} > 0.25$ and log-likelihood > 1, with linear regression line and corresponding R^2 and p-value. Shaded band: 95% CI
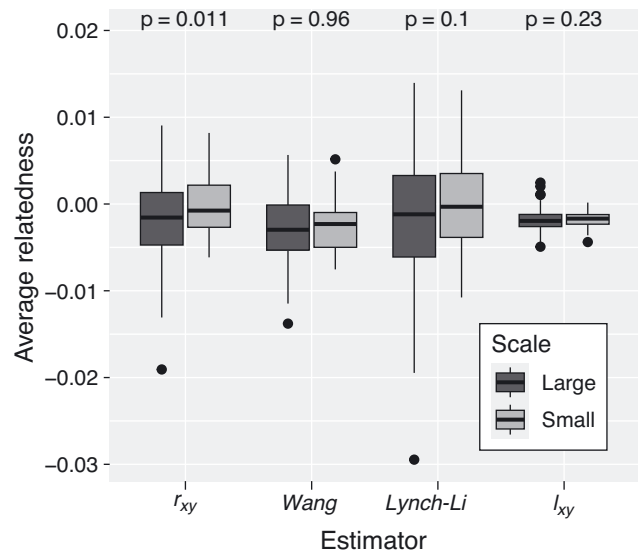

Fig. 5. Average relatedness for 4 commonly used estimators across large-scale and small-scale sites. Boxes range from the first (Q1) to the third quartile (Q3) of the distribution of average relatedness values; horizontal bar across the box: median average relatedness; whiskers extend to calculated minimum and maximum average relatedness (Q1 – 1.5 × interquartile range; Q3 + 1.5 × interquartile range); dots: outliers beyond calculated minima and maxima. The p-values correspond to unpaired *t*-tests with the exception of the Lynch-Ritland estimator l_{xy} (Lynch & Ritland 1999), which corresponds to a Wilcoxon test

hypothesis of significant gene flow in the sampled area, sufficient enough to lead to genetic homogeneity at the spatial scale sampled, and no sampling sites were differentiated, with genetic diversity remaining high and homogeneous throughout the study range.

The absence of genetic differentiation can be explained by several characteristics of *L. pholis*. Unlike other species of comparable habitat and life-history characteristics (i.e. pelagic larval dispersal coupled with limited adult movement) where genetic differentiation was found on smaller scales (*Trypterigion delaisi*: PLD = 16–21 d, Macpherson & Raventós 2006, Schunter et al. 2011; *Salaria pavo*: PLD = 18 d, von Westernhagen 1983, Castilho et al. 2017), *L. pholis* features a longer PLD (57–73 d, Carvalho et al. 2017a). A lack of large-scale (100–500 km) genetic structure has been reported for species with a similar or slightly longer PLD, such as *Sicyopterus aiensis* and *S. sarasini*, which are Vanuatu and New Caledonia endemics, respectively (Lord et al. 2012); or *Awaous guamensis*, *Stenogobius hawaiiensis*, *Lentipes concolor*, and *Sicyopterus stimpsoni*, which are distributed in the Hawaiian Islands (Fitzsimons et al. 1990, Zink et al. 1996, Chubb et al. 1998). For some species, genetic structure only appears at very large scales (*Sicyopterus lagocephalus*, Lord et al. 2012). This might also be the case of *L. pholis*, for which a previous study based on mitochondrial sequencing (CR, 12S, and 16S rDNA) found genetic differentiation of the Azores group, the westernmost distribution range of *L. pholis*, which are found ~1000 km from Madeira, and ~1500 km from mainland Portugal (Stefanni et al. 2006). The use of PLD as a predic-

tor of high dispersal abilities has long been challenged (Weersing & Toonen 2009, Shanks 2009), but re-evaluation of several studies showed a consistent fit between genetic and PLD proxies of dispersal (Selkoe & Toonen 2011). A positive correlation between gene flow and PLD specifically occurs in several blennioid fishes (Riginos & Victor 2001). In addition, the ability of *L. pholis* larvae to disperse over long distances has been shown using otolith chemistry, with estimated dispersal distances superior to 300 km (Carvalho et al. 2017b).

4.2. Weak broad-scale signal of IBD

Both the MSR–Mantel tests using genetic distance and kinship-based modelling approaches challenge the initial assumption of genetic homogeneity at the scale of the Western Iberian Peninsula. MSR–Mantel tests revealed a significant effect of geographic distance in shaping genetic distance for a scale of >500 km when using Nei's genetic distance or F_{ST}^*, suggesting that geographic distance may contribute to genetic differentiation among samples through IBD. This hypothesis was further corrobo-

rated by the regression analysis based on relatedness coefficients when using less stringent cut-off ratios to identify relationships. These results contrast the previous study by Francisco et al. (2011), which spanned a larger scale from the Netherlands to the South of Spain (>1800 km) and did not detect IBD using mtDNA and the S7 nuclear marker. This difference likely stems from the use of distinct methodological approaches and further underlines the utility of both accounting for marker type and using kinship-based approaches in detecting even weak signals of IBD for populations with low genetic divergence (Oleksa 2014, Schunter et al. 2019).

It is worth stressing that the magnitude of the IBD signal remains limited. Although several lines of analysis suggest a negative association between relatedness and geographic distance, the significance of results differ based on the choice of metric or estimator used. The linear regression based on relatedness values yielded negative slopes for all estimators; however, in all cases these slopes were close to zero. As a matter of fact, all but one estimator (Lynch-Ritland l_{xy}) identified no significant relationship between relatedness values and distance. Similarly, average relatedness was slightly but consistently higher among sites distributed within ~50 km compared to broad-scale analysis sites, although this difference was only significant for the Queller-Goodnight estimator r_{xy}. The number of half-sibling relationships inferred also appeared to decrease with distance, and when applying more stringent conditions to select these relationships, this association remained negative but was no longer significant. It is difficult to identify whether this is a result of reducing the overall number of relationships or the specific exclusion of unrelated individuals that had been considered as related at higher thresholds. The fact that the relationships identified with the highest level of confidence were also the closest suggests that truly related individuals are in fact found closer to one another. However, these findings urge us to use caution when interpreting these results, and while relatedness analysis stands as a valuable complement to other population-based methods, using it alone may prove insufficiently robust in weakly related populations.

For Mantel tests based on genetic distance, out of the 4 tests (2 measures of genetic distance and 2 measures of geographic distance), only one involving Nei's genetic distance and least-cost path distance did not detect an IBD signal, while the 3 other tests identified a weak signal of structuring by distance, with r statistics close to zero. This serves to underline the usefulness of testing for multiple genetic distances when using Mantel tests for IBD characterization. Spatial autocorrelation can falsely inflate the rate of significant results when detecting IBD using Mantel tests if not appropriately accounted for. However, there is also evidence that some sampling strategies (e.g. sampling pre-defined populations instead of sampling evenly distributed individuals) can lead to lower levels of IBD detection (Schwartz & McKelvey 2009). Our study adds to the increasing evidence of the benefits of approaching IBD detection through multiple metrics and methods. In spite of the important implications of geographically limited dispersal, many studies investigating population structure still fail to test for IBD, and among the remaining studies, only a small proportion considers a combination of methods to do so (Perez et al. 2018).

Our results indicate that computing least-cost path distances did not seem relevant in improving predictions of relatedness in the study area. This may be due to coastal configuration and the relatively consistent north–south directionality of the sampling sites, resulting in least-cost path distances being similar to straight-line distances, with an average difference of 18 km and a maximum difference of 68 km between the 2 distances (Table S6 in the Supplement). Therefore, this approach may be best suited for study areas featuring discontinuities in the dispersal landscape that would generate larger differences between the least-cost path distances and the straight-line distances (Van Wynsberge et al. 2017).

4.3. Fine-scale connectivity within an MPA network of islands

Connectivity in a network of MPAs is a critical feature guaranteeing effectiveness in protecting species of commercial or conservation interest (Pujolar et al. 2013). Although *L. pholis* is not a target species in the MPAs' conservation strategy, monitoring non-target species can allow assessment of the indirect effectiveness of the MPA, as the species dynamics are directly impacted by its predators, which include the fisheries' target species *Gadus morhua* (Pinnegar & Stafford 2014). In the case of no-take MPAs, such indirect effects (i.e. cascading effects) have been documented, leading to a reduction in the abundance of species not targeted by fisheries (Heyns-Veale et al. 2019), with consequences for population structure and genetic diversity (Allendorf et al. 2008). However, the present study revealed no evidence of such an effect at the scale of the Atlantic Islands of Galicia National Park. Genetic diversity remained

high throughout the 8 sampling sites located within and outside the MPA. In addition, no pattern of IBD was detected, and the relatedness regression analysis did not reveal significant structuring of related individuals by distance, suggesting genetic homogeneity at the spatial scale of ~50 km.

4.4. Geographic distance as a predictor of genetic differentiation

Given the significant but low contribution of geographic distance in explaining relatedness patterns ($R^2 < 4.26\%$), it is likely that factors beyond the scope of our study were better predictors of the distribution of related individuals along the coastline. Exposure to varying oceanographic conditions during the spawning season may provide a better explanation of the difference between geographic and dispersal distances. The shanny *L. pholis* features multiple spawning events during the breeding season (Qasim 1956), which increases the variability of realized geographic distances separating related individuals. As such, larvae from the same year are exposed to different oceanic conditions due to important seasonal variability in Northeast Atlantic large-scale circulation (Wooster et al. 1976, Saunders 1982, Álvarez-Salgado et al. 2003), therefore potentially decoupling larval dispersal distance from geographic distance. Siegel et al. (2008) also proposed that given the large variability of coastal circulation, alongshore larval transport and settlement in nearshore species are inherently stochastic, constituting a source of unresolvable noise in recruitment patterns, which may account for a large part of the observed distribution of related individuals in *L. pholis*.

Correlation between gene flow and geographic distance is well documented for several marine fish species presenting high dispersal capabilities, yet the observed patterns of genetic differentiation according to distance are highly variable. A recurring pattern of increase in gene flow over smaller distances has been found in a number of species (Waples 1987, Doherty et al. 1995), often depending on the observed scale (*G. morhua*, Pogson et al. 1995, Pogson et al. 2001; *Sardina pilchardus*, Laurent et al. 2007; *Acanthurus triostegus*, Planes & Fauvelot 2002). This finding is also applicable to *L. pholis*, for which we documented evidence of higher gene flow at a smaller spatial scale. However, the observation that larger spatial scales lead to lesser gene flow may not hold true across the entire species' distribution range. In the case of *A.*

triostegus, Planes & Fauvelot (2002) described the existence of 2 distinct processes driving genetic differentiation at the scale of the Pacific: vicariance and IBD. This may be comparable to previously observed patterns of genetic differentiation in *L. pholis*, where the genetically isolated population of the Azores has been hypothesized to result from divergent population histories (Stefanni et al. 2006).

5. CONCLUSIONS

Our combination of population-based and kinship-based methods indicates that *Lipophrys pholis* displays high genetic diversity and a high level of gene flow along the Western Iberian Peninsula coastline, generating genetic homogeneity at least at the scale of the Atlantic Islands National Park, as well as a weak pattern of IBD appearing at the larger scale of >500 km. These results stress the importance of accounting for spatial scale in genetic studies, as 2 different patterns emerged according to the studied area: fine-scale relative homogeneity (<50 km) and large-scale IBD. This can be useful in the context of designing MPA networks: accurately assessing the magnitude of IBD for keystone species can help determine a maximum distance separating MPAs, so as to maintain gene flow above a certain threshold (Shanks et al. 2003, Palumbi 2004, Durrant et al. 2014). The present study ultimately reinforces the utility of associating multiple approaches in assessing genetic patterns in species with high gene flow, underlining both the challenges associated with studying these species as well as the need for careful interpretation in these cases. Larger sample sizes and a greater number of genetic markers, together with the possible use of single nucleotide polymorphisms (Bonin et al. 2007, Sunde et al. 2020), may be necessary to provide a better understanding of fundamental evolutionary processes shaping weakly differentiated species' distributions, population and community dynamics.

LITERATURE CITED

Allendorf FW, England PR, Luikart G, Ritchie PA, Ryman N (2008) Genetic effects of harvest on wild animal populations. Trends Ecol Evol 23:327–337

Almada V, Barata E, Gonçalves E, Oliveira R (1990) On the breeding season of *Lipophrys pholis* (Pisces: Blenniidae) at Arrábida, Portugal. J Mar Biol Assoc UK 70:913–916

Almeida AJ (1985) Clef pour la détermination des Blenniidae et Tripterygiidae marin du Portugal Continental, Açores et Madère. Bocagiana 87:1–14

Álvarez-Salgado XA, Figueiras FG, Pérez FF, Groom S and others (2003) The Portugal coastal counter current off NW Spain: new insights on its biogeochemical variability. Prog Oceanogr 56:281–321

Anderson EC (2023) CKMRsim: inference of pairwise relationships using likelihood ratios. R package version 0.1.2.999. https://github.com/eriqande/CKMRsim/tree/master

Baetscher DS, Clemento AJ, Ng TC, Anderson EC, Garza JC (2018) Microhaplotypes provide increased power from short-read DNA sequences for relationship inference. Mol Ecol Resour 18:296–305

Baetscher DS, Anderson EC, Gilbert-Horvath EA, Malone DP, Saarman ET, Carr MH, Garza JC (2019) Dispersal of a nearshore marine fish connects marine reserves and adjacent fished areas along an open coast. Mol Ecol 28: 1611–1623

Balloux F, Goudet J (2002) Statistical properties of population differentiation estimators under stepwise mutation in a finite island model. Mol Ecol 11:771–783

Banks SC, Piggott LMP, Williamson JE, Bové U, Holbrook NJ, Beheregaray LB (2007) Oceanic variability and coastal topography shape genetic structure in a long-dispersing sea urchin. Ecology 88:3055–3064

Barton K (2020) MuMIn: multi-model inference. R package version 1.43.17. https://CRAN.R-project.org/package=MuMIn

Beger M, Linke S, Watts M, Game E, Treml E, Ball I, Possingham H (2010) Incorporating asymmetric connectivity into spatial decision making for conservation. Conserv Lett 3:359–368

Beger M, McGowan J, Treml EA, Green AL and others (2015) Integrating regional conservation priorities for multiple objectives into national policy. Nat Commun 6: 8208

Belkhir K, Borsam P, Chikhi L, Raufaste N, Bonhomme F (1996) Genetix 4.05, logiciel sous Windows TM pour la génétique des populations. Laboratoire Génome, Populations, Interactions, CNRS UMR 5000. Université de Montpellier II, Montpellier

Blouin MS, Parsons M, Lacaille V, Lotz S (1996) Use of microsatellite loci to classify individuals by relatedness. Mol Ecol 5:393–401

Bonhomme F, Planes S (2000) Some evolutionary arguments about what maintains the pelagic interval in reef fishes. Environ Biol Fishes 59:365–383

Bonin A, Ehrich D, Manel S (2007) Statistical analysis of amplified fragment length polymorphism data: a toolbox for molecular ecologists and evolutionists. Mol Ecol 16: 3737–3758

Botsford LW, White JW, Coffroth MA, Paris CB and others (2009) Connectivity and resilience of coral reef metapopulations in marine protected areas: matching empirical efforts to predictive needs. Coral Reefs 28:327–337

Brooks M, Kristensen K, van Benthem K, Magnusson A and others (2017) GlmmTMB balances speed and flexibility among packages for zero-inflated generalized linear mixed modeling. R J 9:378–400

Buston PM, Bogdanowicz SM, Wong A, Harrison RG (2007) Are clownfish groups composed of close relatives? An analysis of microsatellite DNA variation in *Amphiprion percula*. Mol Ecol 16:3671–3678

Buston PM, Fauvelot C, Wong MYL, Planes S (2009) Genetic relatedness in groups of the humbug damselfish *Dascyllus aruanus*: small, similar-sized individuals may be close kin. Mol Ecol 18:4707–4715

Carvalho MG, Moreira C, Queiroga H, Santos PT, Correia AT (2017a) Pelagic larval duration, size at settlement and coastal recruitment of the intertidal blenny *Lipophrys pholis*. J Mar Biol Assoc UK 97:197–205

Carvalho MG, Moreira C, Cardoso JFMF, Brummer GJA and others (2017b) Movement, connectivity and population structure of the intertidal fish *Lipophrys pholis* as revealed by otolith oxygen and carbon stable isotopes. Mar Biol Res 13:764–773

Carvalho MG, Moreira C, Queiroga H, Santos PT, Correia AT (2017c) Age, growth and sex of the shanny, *Lipophrys pholis* (Linnaeus, 1758) (Teleostei, Blenniidae), from the NW coast of Portugal. J Appl Ichthyology 33:242–251

Castilho R, Cunha RL, Faria C, Velasco EM, Robalo JI (2017) Asymmetrical dispersal and putative isolation-by-distance of an intertidal blenniid across the Atlantic–Mediterranean divide. PeerJ 5:e3195

Christie MR, Johnson DW, Stallings CD, Hixon MA (2010) Self-recruitment and sweepstakes reproduction amid extensive gene flow in a coral-reef fish. Mol Ecol 19: 1042–1057

Chubb AL, Zink RM, Fitzsimons JM (1998) Patterns of mtDNA variation in Hawaiian freshwater fishes: the phylogeographic consequences of amphidromy. J Hered 89: 8–16

Cowen RK, Sponaugle S (2009) Larval dispersal and marine population connectivity. Annu Rev Mar Sci 1:443–466

Cowen RK, Lwiza KMM, Sponaugle S, Paris CB, Olson DB (2000) Connectivity of marine populations: open or closed? Science 287:857–859

Cowen RK, Paris CB, Srinivasan A (2006) Scaling of connectivity in marine populations. Science 311:522–527

Cowen RK, Gawarkiewicz G, Pineda J, Thorrold SR, Werner FE (2007) Population connectivity in marine systems: an overview. Oceanography 20:14–21

Crabot J, Clappe S, Dray S, Datry T (2019) Testing the Mantel statistic with a spatially-constrained permutation procedure. Methods Ecol Evol 10:532–540

Csilléry K, Johnson T, Beraldi D, Clutton-Brock T and others (2006) Performance of marker-based relatedness estimators in natural populations of outbred vertebrates. Genetics 173:2091–2101

D'Aloia CC, Xuereb A, Fortin MJ, Bogdanowicz SM, Buston PM (2018) Limited dispersal explains the spatial distribution of siblings in a reef fish population. Mar Ecol Prog Ser 607:143–154

Dalongeville A, Andrello M, Mouillot D, Lobreaux S and others (2018) Geographic isolation and larval dispersal shape seascape genetic patterns differently according to spatial scale. Evol Appl 11:1437–1447

Doherty PJ, Planes S, Mather P (1995) Gene flow and larval duration in seven species of fish from the Great Barrier Reef. Ecology 76:2373–2391

Dray S, Bauman D, Blanchet G, Borcard D and others (2022) adespatial: multivariate multiscale spatial analysis. R package version 0.3-20. https://CRAN.R-project.org/package=adespatial

Dunne J (1977) The biology of the shanny, *Blennius pholis* L. (Pisces) at Carna, Connemara. Proc R Ir Acad 77: 207–226

Durrant HMS, Burridge CP, Kelaher BP, Barrett NS, Edgar GJ, Coleman MA (2014) Implications of macroalgal isolation by distance for networks of marine protected areas. Conserv Biol 28:438–445

Earl DA, vonHoldt BM (2012) STRUCTURE HARVESTER: a website and program for visualizing STRUCTURE output and implementing the Evanno method. Conserv Genet Resour 4:359–361

Escoda L, González-Esteban J, Gómez A, Castresana J (2017) Using relatedness networks to infer contemporary dispersal: application to the endangered mammal *Galemys pyrenaicus*. Mol Ecol 26:3343–3357

Evanno G, Regnaut S, Goudet J (2005) Detecting the number of clusters of individuals using the software STRUCTURE: a simulation study. Mol Ecol 14:2611–2620

Faria C, Almada V (2001) Agonistic behaviour and control of access to hiding places in two intertidal blennies, *Lipophrys pholis* and *Coryphoblennius galerita* (Pisces: Blenniidae). Acta Ethol 4:51–58

Faria C, Almada VC, Goncalves EJ (1996) Juvenile recruitment, growth and maturation of *Lipophrys pholis* (Pisces: Blenniidae), from the west coast of Portugal. J Fish Biol 49:727–730

Fitzsimons JM, Zink RM, Nishimoto RT (1990) Genetic variation in the Hawaiian stream goby, *Lentipes concolor*. Biochem Syst Ecol 18:81–83

Francisco S, Robalo J (2015) Genetic structure and effective population size through time: a tale on two coastal marine species with contrasting life-history patterns. J Phylogenetics Evol Biol 3:155

Francisco SM, Robalo JI (2020) Time matters: genetic composition and evaluation of effective population size in temperate coastal fish species. PeerJ 8:e9098

Francisco SM, Vieira MN, Almada VC (2006) Genetic structure and historical demography of the shanny *Lipophrys pholis* in the Portuguese coast based on mitochondrial DNA analysis. Mol Phylogenet Evol 39: 288–292

Francisco SM, Faria C, Lengkeek W, Vieira MN, Velasco EM, Almada VC (2011) Phylogeography of the shanny *Lipophrys pholis* (Pisces: Blenniidae) in the NE Atlantic records signs of major expansion event older than the last glaciation. J Exp Mar Biol Ecol 403:14–20

Gerlach G, Atema J, Kingsford MJ, Black KP, Miller-Sims V (2007) Smelling home can prevent dispersal of reef fish larvae. Proc Natl Acad Sci USA 104:858–863

Gibson RN (1982) Recent studies on the biology of intertidal fishes. Oceanogr Mar Biol Annu Rev 20:363–414

Gotelli NJ, McCabe DJ (2002) Species co-occurrence: a meta-analysis of JM Diamond's assembly rules model. Ecology 83:2091–2096

Guillot G, Rousset F (2013) Dismantling the Mantel tests. Methods Ecol Evol 4:336–344

Harrison HB, Saenz-Agudelo P, Planes S, Jones GP, Berumen ML (2013a) On minimizing assignment errors and the trade-off between false positives and negatives in parentage analysis. Mol Ecol 22:5738–5742

Harrison HB, Saenz-Agudelo P, Planes S, Jones GP, Berumen ML (2013b) Relative accuracy of three common methods of parentage analysis in natural populations. Mol Ecol 22:1158–1170

Heyns-Veale ER, Bernard ATF, Götz A, Mann BQ, Maggs JQ, Smith MKS (2019) Community-wide effects of protection reveal insights into marine protected area effectiveness for reef fish. Mar Ecol Prog Ser 620:99–117

Hijmans RJ (2021a) geosphere: sperical trigonometry. R package version 1.5-14. https://CRAN.R-project.org/package=geosphere

Hijmans RJ (2021b) raster: geographic data analysis and modeling. R package version 3.5-2. https://CRAN.R-project.org/package=raster

Hughes TP, Baird AH, Bellwood DR, Card M and others (2003) Climate change, human impacts, and the resilience of coral reefs. Science 301:929–933

Huyghe F, Kochzius M (2018) Sea surface currents and geographic isolation shape the genetic population structure of a coral reef fish in the Indian Ocean. PLOS ONE 13: e0193825

Iacchei M, Ben-Horin T, Selkoe KA, Bird CE, García-Rodríguez FJ, Toonen RJ (2013) Combined analyses of kinship and F_{ST} suggest potential drivers of chaotic genetic patchiness in high gene-flow populations. Mol Ecol 22:3476–3494

Jeannot LL, Mouronvalle C, Peyran C, Blanco A, Planes S (2022) Development of 27 new microsatellite markers for the shanny *Lipophrys pholis*. Mol Biol Rep 49:9051–9057

Jones AG, Small CM, Paczolt KA, Ratterman NL (2010) A practical guide to methods of parentage analysis. Mol Ecol Resour 10:6–30

Jorge PE, Almada F, Gonçalves AR, Duarte-Coelho P, Almada VC (2012) Homing in rocky intertidal fish: Are *Lipophrys pholis* L. able to perform true navigation? Anim Cogn 15:1173–1181

Knutsen H, Jorde PE, Gonzalez EB, Robalo J, Albretsen J, Almada V (2013) Climate change and genetic structure of leading edge and rear end populations in a northwards shifting marine fish species, the corkwing wrasse (*Symphodus melops*). PLOS ONE 8:e67492

Kraemer P, Gerlach G (2017) Demerelate: calculating interindividual relatedness for kinship analysis based on codominant diploid genetic markers using R. Mol Ecol Resour 17:1371–1377

Landguth EL, Cushman SA, Schwartz MK, McKelvey KS, Murphy M, Luikart G (2010) Quantifying the lag time to detect barriers in landscape genetics. Mol Ecol 19: 4179–4191

Laurent V, Caneco B, Magoulas A, Planes S (2007) Isolation by distance and selection effects on genetic structure of sardines *Sardina pilchardus* Walbaum. J Fish Biol 71: 1–17

Legendre P, Fortin MJ, Borcard D (2015) Should the Mantel test be used in spatial analysis? Methods Ecol Evol 6: 1239–1247

Leis JM (2007) Behaviour as input for modelling dispersal of fish larvae: behaviour, biogeography, hydrodynamics, ontogeny, physiology and phylogeny meet hydrography. Mar Ecol Prog Ser 347:185–193

Li CC, Weeks DE, Chakravarti A (1993) Similarity of DNA fingerprints due to chance and relatedness. Hum Hered 43:45–52

Lloyd MW, Campbell L, Neel MC (2013) The power to detect recent fragmentation events using genetic differentiation methods. PLOS ONE 8:e63981

Lord C, Lorion J, Dettai A, Watanabe S, Tsukamoto K, Cruaud C, Keith P (2012) From endemism to widespread distribution: phylogeography of three amphidromous *Sicyopterus* species (Teleostei: Gobioidei: Sicydiinae). Mar Ecol Prog Ser 455:269−285

Lynch M, Ritland K (1999) Estimation of pairwise relatedness with molecular markers. Genetics 152:1753−1766

Macpherson E, Raventos N (2006) Relationship between pelagic larval duration and geographic distribution of Mediterranean littoral fishes. Mar Ecol Prog Ser 327:257−265

Martins J, Almada F, Gonçalves A, Duarte-Coelho P, Jorge PE (2017) Home sweet home: evidence for nest-fidelity in the rocky intertidal fish, the shanny *Lipophrys pholis*. J Fish Biol 90:156−166

Melero Y, Oliver MK, Lambin X (2017) Relationship type affects the reliability of dispersal distance estimated using pedigree inferences in partially sampled populations: a case study involving invasive American mink in Scotland. Mol Ecol 26:4059−4071

Milligan BG (2003) Maximum-likelihood estimation of relatedness. Genetics 163:1153−1167

Monteiro NM, Quinteira SM, Silva K, Vleira MN, Almada VC (2005) Diet preference reflects the ontogenetic shift in microhabitat use in *Lipophrys pholis*. J Fish Biol 67:102−113

Nance HA, Klimley P, Galván-Magaña F, Martínez-Ortíz J, Marko PB (2011) Demographic processes underlying subtle patterns of population structure in the scalloped hammerhead shark, *Sphyrna lewini*. PLOS ONE 6:e21459

Nei M (1972) Genetic distance between populations. Am Nat 106:283−292

Oleksa A (2014) Weak isolation by distance in *Diaperis boleti*, a fungivorous saproxylic beetle. J Insect Sci 14:1−12

Oliehoek PA, Windig JJ, van Arendonk JAM, Bijma P (2006) Estimating relatedness between individuals in general populations with a focus on their use in conservation programs. Genetics 173:483−496

Paetkau D, Calvert W, Stirling I, Strobeck I (1995) Microsatellite analysis of population structure in Canadian polar bears. Mol Ecol 4:347−354

Palsbøll PJ, Peery Z, Bérubé M (2010) Detecting populations in the 'ambiguous' zone: kinship-based estimation of population structure at low genetic divergence. Mol Ecol Resour 10:797−805

Palumbi SR (2003) Population genetics, demographic connectivity, and the design of marine reserves. Ecol Appl 13:S146−S158

Palumbi SR (2004) Marine reserves and ocean neighborhoods: the spatial scale of marine populations and their management. Annu Rev Environ Resour 29:31−68

Paris CB, Cowen RK (2004) Direct evidence of a biophysical retention mechanism for coral reef fish larvae. Limnol Oceanogr 49:1964−1979

Peakall R, Smouse PE (2006) Genalex 6: genetic analysis in Excel. Population genetic software for teaching and research. Mol Ecol Notes 6:288−295

Peakall R, Smouse PE (2012) GenALEx 6.5: genetic analysis in Excel. Population genetic software for teaching and research—an update. Bioinformatics 28:2537−2539

Peery MZ, Beissinger SR, House RF, Bérubé M, Hall LA, Sellas A, Palsbøll PJ (2008) Characterizing source–sink dynamics with genetic parentage assignments. Ecology 89:2746−2759

Perez MF, Franco FF, Bombonato JR, Bonatelli IAS and others (2018) Assessing population structure in the face of isolation by distance: Are we neglecting the problem? Divers Distrib 24:1883−1889

Pew J, Muir PH, Wang J, Frasier TR (2015) related: an R package for analysing pairwise relatedness from codominant molecular markers. Mol Ecol Resour 15:557−561

Pinnegar J, Stafford R (2014) DAPSTOM—an integrated database & portal for fish stomach records. Centre for Environment, Fisheries & Aquaculture Science, Suffolk. https://data.cefas.co.uk/view/21715

Planes S, Fauvelot C (2002) Isolation by distance and vicariance drive genetic structure of a coral reef fish in the Pacific Ocean. Evolution 56:378−399

Planes S, Jones GP, Thorrold S (2009) Larval dispersal connects fish populations in a network of marine protected areas. Proc Natl Acad Sci USA 106:5693−5697

Pogson GH, Mesa KA, Boutilier RG (1995) Genetic population structure and gene flow in the Atlantic cod *Gadus morhua*: a comparison of allozyme and nuclear RFLP loci. Genetics 139:375−385

Pogson GH, Taggart CT, Mesa KA, Boutilier RG (2001) Isolation by distance in the Atlantic cod, *Gadus morhua*, at large and small geographic scales. Evolution 55:131−146

Pritchard JK, Stephens M, Donnelly P (2000) Inference of population structure using multilocus genotype data. Genetics 155:945−959

Pujolar JM, Schiavina M, Di Franco A, Melià P and others (2013) Understanding the effectiveness of marine protected areas using genetic connectivity patterns and Lagrangian simulations. Divers Distrib 19:1531−1542

Qasim SZ (1956) The spawning habits and embryonic development of the shanny (*Blennius pholis* L.). Proc Zool Soc Lond 127:79−93

Queller DC, Goodnight KF (1989) Estimating relatedness using genetic markers. Evolution 43:258−275

R Core Team (2020) R: a language and environment for statistical computing. R Foundation for Statistical Computing, Vienna

Raufaste N, Bonhomme F (2000) Properties of bias and variance of two multiallelic estimators of F_{ST}. Theor Popul Biol 57:285−296

Rickman S, Dulvy N, Jennings S, Reynolds J (2000) Recruitment variation related to fecundity in marine fishes. Can J Fish Aquat Sci 57:116−124

Riginos C, Victor BC (2001) Larval spatial distributions and other early life-history characteristics predict genetic differentiation in eastern Pacific blennioid fishes. Proc R Soc B 268:1931−1936

Ritland K (1996a) A marker-based method for inferences about quantitative inheritance in natural populations. Evolution 50:1062−1073

Ritland K (1996b) Estimators for pairwise relatedness and individual inbreeding coefficients. Genet Res 67:175−185

Robertson A, Hill WG (1984) Deviations from Hardy-Weinberg proportions: sampling variances and use in estimation of inbreeding coefficients. Genetics 107:703−718

Rousset F (1997) Genetic differentiation and estimation of gene flow from *F*-statistics under isolation by distance. Genetics 145:1219−1228

Rueger T, Harrison HB, Buston PM, Gardiner NM, Berumen ML, Jones GP (2020) Natal philopatry increases relatedness within groups of coral reef cardinalfish. Proc R Soc B 287:20201133

Rueger T, Buston PM, Bogdanowicz SM, Wong MY (2021) Genetic relatedness in social groups of the emerald coral goby *Paragobiodon xanthosoma* creates potential for weak kin selection. Mol Ecol 30:1311–1321

Saenz-Agudelo P, Jones GP, Thorrold SR, Planes S (2009) Estimating connectivity in marine populations: an empirical evaluation of assignment tests and parentage analysis under different gene flow scenarios. Mol Ecol 18: 1765–1776

Sakamoto Y, Ishiguro M, Kitagawa G (1986) Akaike information criterion statistics. KTK Scientific Publishers, Tokyo

Saunders PM (1982) Circulation in the eastern North Atlantic. J Mar Res 40:641–657

Schunter C, Carreras-Carbonell J, Macpherson E, Tintoré J and others (2011) Matching genetics with oceanography: directional gene flow in a Mediterranean fish species. Mol Ecol 20:5167–5181

Schunter C, Pascual M, Garza JC, Raventos N, Macpherson E (2014) Kinship analyses identify fish dispersal events on a temperate coastline. Proc R Soc B 281:20140556

Schunter C, Pascual M, Raventos N, Garriga J, Garza JC, Bartumeus F, Macpherson E (2019) A novel integrative approach elucidates fine-scale dispersal patchiness in marine populations. Sci Rep 9:10796

Schwartz MK, McKelvey KS (2009) Why sampling scheme matters: the effect of sampling scheme on landscape genetic results. Conserv Genet 10:441–452

Selkoe KA, Toonen RJ (2011) Marine connectivity: a new look at pelagic larval duration and genetic metrics of dispersal. Mar Ecol Prog Ser 436:291–305

Séré M, Thévenon S, Belem AMG, De Meeûs T (2017) Comparison of different genetic distances to test isolation by distance between populations. Heredity 119:55–63

Shanks AL (2009) Pelagic larval duration and dispersal distance revisited. Biol Bull 216:373–385

Shanks AL, Grantham BA, Carr MH (2003) Propagule dispersal distance and the size and spacing of marine reserves. Ecol Appl 13:159–169

Siegel DA, Mitarai S, Costello CJ, Gaines SD, Kendall BE, Warner RR, Winters KB (2008) The stochastic nature of larval connectivity among nearshore marine populations. Proc Natl Acad Sci USA 105:8974–8979

Sinnott RW (1984) Virtues of the haversine. Sky Telescope 68:158–159

Slatkin M (1987) Gene flow and the geographic structure of natural populations. Science 236:787–792

Slatkin M (1993) Isolation by distance in equilibrium and non-equilibrium populations. Evolution 47:264–279

Stefanni S, Domingues V, Bouton N, Santos RS, Almada F, Almada V (2006) Phylogeny of the shanny, *Lipophrys pholis*, from the NE Atlantic using mitochondrial DNA markers. Mol Phylogenet Evol 39:282–287

Sunde J, Yıldırım Y, Tibblin P, Forsman A (2020) Comparing the performance of microsatellites and RADseq in population genetic studies: analysis of data for pike (*Esox lucius*) and a synthesis of previous studies. Front Genet 11:218

Szpiech ZA, Jakobsson M, Rosenberg NA (2008) ADZE: a rarefaction approach for counting alleles private to combinations of populations. Bioinformatics 24: 2498–2504

Taylor HR (2015) The use and abuse of genetic marker-based estimates of relatedness and inbreeding. Ecol Evol 5:3140–3150

Thomas SC (2005) The estimation of genetic relationships using molecular markers and their efficiency in estimating heritability in natural populations. Philos Trans R Soc Lond B Biol Sci 360:1457–1467

Treml EA, Roberts JJ, Chao Y, Halpin PN, Possingham HP, Riginos C (2012) Reproductive output and duration of the pelagic larval stage determine seascape-wide connectivity of marine populations. Integr Comp Biol 52:525–537

Van de Casteele T, Galbusera P, Matthysen E (2001) A comparison of microsatellite-based pairwise relatedness estimators. Mol Ecol 10:1539–1549

van Etten J (2017) R package gdistance: distances and routes on geographical grids. J Stat Softw 76:1–21

van Oosterhout C, Hutchinson WF, Wills DPM, Shipley P (2004) MICRO-CHECKER: software for identifying and correcting genotyping errors in microsatellite data. Mol Ecol Notes 4:535–538

Van Wynsberge S, Andréfouët S, Gaertner-Mazouni N, Tiavouane J and others (2017) Considering reefscape configuration and composition in biophysical models advance seascape genetics. PLOS ONE 12:e0178239

von Westernhagen H (1983) Observations on the reproductive and larval biology of *Blennius pavo* (Pisces: Teleostei). Helgol Meeresunters 36:323–335

Wang J (2002) An estimator for pairwise relatedness using molecular markers. Genetics 160:1203–1215

Wang J (2007) Triadic IBD coefficients and applications to estimating pairwise relatedness. Genet Res 89:135–153

Wang J (2009) A new method for estimating effective population sizes from a single sample of multilocus genotypes. Mol Ecol 18:2148–2164

Waples RS (1987) A multispecies approach to the analysis of gene flow in marine shore fishes. Evolution 41:385–400

Weersing K, Toonen RJ (2009) Population genetics, larval dispersal, and connectivity in marine systems. Mar Ecol Prog Ser 393:1–12

Weir BS, Cockerham CC (1984) Estimating *F*-statistics for the analysis of population structure. Evolution 38: 1358–1370

White C, Selkoe KA, Watson J, Siegel DA, Zacherl DC, Toonen RJ (2010) Ocean currents help explain population genetic structure. Proc R Soc B 277:1685–1694

Wilson AJ, Ferguson MM (2002) Molecular pedigree analysis in natural populations of fishes: approaches, applications, and practical considerations. Can J Fish Aquat Sci 59:1696–1707

Wooster WS, Bakun A, McLain DR (1976) Seasonal upwelling cycle along the eastern boundary of the North Atlantic. J Mar Res 34:131–141

Wright S (1949) The genetical structure of populations. Ann Eugen 15:323–354

Zander CD (1986) Blenniidae. In: Whitehead PJP, Bauchot ML, Hureau JC, Nielsen J, Tortonese E (eds) Fishes of the North-eastern Atlantic and the Mediterranean, Vol 3. UNESCO, Paris, p 1096–1112

Zink RM, Fitzsimons JM, Dittmann DL, Reynolds DR, Nishimoto RT (1996) Evolutionary genetics of Hawaiian freshwater fish. Copeia 1996:330–335